Mineralogical Magazine, February 2016, Vol. 80(1), pp. 175–186

Ferrostalderite, $CuFe_2TlAs_2S_6$, a new mineral from Lengenbach, Switzerland: occurrence, crystal structure, and emphasis on the role of iron in sulfosalts

Cristian Biagioni[1,*], Luca Bindi[2], Fabrizio Nestola[3], Ralph Cannon[4], Philippe Roth[5] and Thomas Raber[6]

[1] Dipartimento di Scienze della Terra, Università di Pisa, Via Santa Maria, 53, I-56126 Pisa, Italy
[2] Dipartimento di Scienze della Terra, Università degli Studi di Firenze, Via G. La Pira, 4, I-50121 Firenze, Italy
[3] Dipartimento di Geoscienze, Università di Padova, Via Gradenigo, 6, I-35131 Padova, Italy
[4] FGL (Forschungsgemeinschaft Lengenbach), Breite Steine, CH-3996 Binn, Switzerland
[5] FGL (Forschungsgemeinschaft Lengenbach), Ilanzhofweg 2, CH-8057 Zurich, Switzerland
[6] FGL (Forschungsgemeinschaft Lengenbach), Edith-Stein-Str. 9, D-79110 Freiburg, Germany

[*Received 25 February 2015; Accepted 30 March 2015; Associate Editor: Ed Grew*]

ABSTRACT

The new mineral species ferrostalderite, $CuFe_2TlAs_2S_6$, was discovered in the Lengenbach quarry, Binn Valley, Wallis, Switzerland. It occurs as minute, metallic, black, equant to prismatic crystals, up to 50 μm, associated with dolomite, realgar, baumhauerite (?) and pyrite. Minimum and maximum reflectance data for COM wavelengths in air are [λ (nm): *R* (%)]: 471.1: 24.2/25.4; 548.3: 23.7/24.7; 586.6: 22.9/23.8; 652.3: 21.0/22.0. Electron microprobe analyses give (wt.%): Cu 6.24(25), Ag 4.18(9), Fe 9.95(83), Zn 4.46(91), Hg 1.22(26), Tl 26.86(62), As 19.05(18), Sb 0.63(6), S 25.39(47), total 97.98(72). On the basis of 12 atoms per formula unit, the chemical formula of ferrostalderite is $Cu_{0.75(2)}Ag_{0.30(1)}Fe_{1.36(10)}Zn_{0.52(11)}Hg_{0.05(1)}Tl_{1.00(1)}[As_{1.94(4)}Sb_{0.04(1)}]_{\Sigma 1.98(4)}S_{6.04(4)}$. The new mineral is tetragonal, space group $I\bar{4}2\,m$, with $a = 9.8786(5)$, $c = 10.8489(8)$ Å, $V = 1058.71(11)$ Å^3, $Z = 4$. The main diffraction lines of the calculated powder diagram are [*d* (in Å), intensity, *hkl*]: 4.092, 70, 211; 3.493, 23, 220; 3.396, 35, 103; 3.124, 17, 310; 2.937, 100, 222; 2.656, 19, 321; 2.470, 19, 400; 2.435, 33, 303. The crystal structure of ferrostalderite has been refined by X-ray single-crystal data to a final $R_1 = 0.050$, on the basis of 1169 reflections with $F_0 > 4\sigma(F_0)$. It shows a three dimensional framework of (Cu,Fe)-centred tetrahedra (1 *M*1 + 2 *M*2), with channels parallel to [001] hosting disymmetric TlS_6 and $(As,Sb)S_3$ polyhedra. Ferrostalderite is derived from its isotype stalderite $^{M1}Cu^{M2}Zn_2TlAs_2S_6$ through the homovalent substitution $^{M2}Zn^{2+} \rightarrow {}^{M2}Fe^{2+}$. The ideal crystal-chemical formula of ferrostalderite is $^{M1}Cu^{M2}Fe_2TlAs_2S_6$.

Keywords: ferrostalderite, new mineral, sulfosalt, thallium, copper, iron, arsenic, crystal structure, Lengenbach, Binn Valley, Switzerland.

Introduction

Mineralogical studies carried out on thallium-bearing mineralizations from Lengenbach, Binn Valley, Switzerland, and Monte Arsiccio mine, Apuan Alps, Tuscany, Italy, allowed the revision of the crystal chemistry of the routhierite isotypic series, as defined by Biagioni *et al*. (2014*b*), and the description of two new mineral species, arsiccioite, $AgHg_2TlAs_2S_6$ (Biagioni *et al*., 2014*b*), and its Zn isotype ralphcannonite, $AgZn_2TlAs_2S_6$ (Bindi *et al*., 2015*b*). During energy dispersive spectrometry (EDS) screening of a suite of specimens collected in the Lengenbach quarry, Ag-rich and Fe-rich stalderite-like phases were identified in 2013. The former were later identified as the new mineral ralphcannonite (Bindi *et al*., 2015*b*), whereas crystallographic studies and chemical

*E-mail: biagioni@dst.unipi.it
DOI: 10.1180/minmag.2015.079.7.10

© 2016 The Mineralogical Society

analyses allowed us to describe the Fe-rich phase as the new mineral ferrostalderite. The mineral and its name have been approved by the Commission on New Minerals, Nomenclature and Classification of the International Mineralogical Association (CNMNC-IMA) (2014-090, Bindi *et al.*, 2015*a*). The holotype specimen of ferrostalderite is deposited in the mineralogical collection of the Museo di Storia Naturale, Università degli Studi di Firenze, Via G. La Pira 4, Florence, Italy, under catalogue number 3148/I. The name indicates that this new phase is the Fe isotype of stalderite, $CuZn_2TlAs_2S_6$. This paper presents the definition, occurrence, and crystal structure of the new mineral species ferrostalderite, and discusses its relationships with the other members of the routhierite isotypic series.

Occurrence and mineral description

The Lengenbach quarry (latitude 46°21′54″N, longitude 8°13′15″E) exploits a Triassic dolostone stratigraphically overlying the gneiss basement at the northern front of the Monte Leone Nappe, belonging to the Penninic Domain of the Alps. These rocks have undergone upper greenschist – lower amphibolite metamorphism. The dolostone formation is 240 m thick at Lengenbach; mineralization occurs in the uppermost part of this dolostone sequence, close to the contact with the stratigraphically overlying Jurassic to Lower Cretaceous *Bündnerschiefer*. Hofmann and Knill (1996) recognized four major types of mineralization: (1) stratiform layers of pyrite with minor galena, sphalerite and xenomorphic sulfosalts; (2) massive to interstitial sulfosalt accumulations; (3) discordant sulfosalt and sulfide veins; and (4) idiomorphic crystals within druses and open fissures. Ferrostalderite was discovered in the second type of mineralization, roughly corresponding to the so-called 'Zone 1' of Graeser *et al*. (2008). The specimen studied was mined in 1999 by the *Interessengemeinschaft Lengenbach* (the then active Lengenbach syndicate) on the third level of the quarry.

Physical and optical properties

Ferrostalderite was observed as black, equant to prismatic euhedral crystals; on the basis of scanning electron microscopy images (Fig. 1) the dominant forms could be the prism {110} and the bipyramid {101}, in agreement with the crystal forms given by Graeser *et al*. (1995) for stalderite. Ferrostalderite is brittle, with an irregular fracture. Its streak is black and the lustre is metallic. Owing to the rarity and the small size of the available crystals, the microhardness was not measured. In plane-polarized incident light, ferrostalderite is dark grey in colour. Under crossed polars, it is weakly anisotropic, with yellowish to bluish rotation tints. Internal reflections are very weak and there is no optical evidence of growth zonation. Reflectance measurements were performed in air using an MPM-200 Zeiss microphotometer equipped with an MSP-20 system processor on a Zeiss Axioplan ore microscope. The filament temperature was ~3350 K. An interference filter was adjusted, in turn, to select four wavelengths (approximating those recommended by the Commission on Ore Mineralogy of the IMA) for measurement (471.1, 548.3, 586.6 and 652.3 nm).

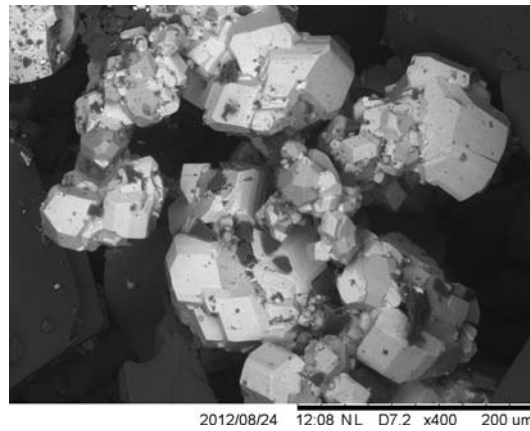

FIG. 1. Scanning electron microscope image of ferrostalderite (light grey), as equant crystals on dolomite (dark grey).

Readings were taken for specimen and standard (SiC) maintained under the same focus conditions. The diameter of the circular measuring area was 0.1 mm. Reflectance percentages for R_{min} and R_{max} are 24.2, 25.4 (471.1 nm), 23.7, 24.7 (548.3 nm), 22.9, 23.8 (586.6 nm) and 21.0, 22.0 (652.3 nm), respectively. Owing to the small amount of pure material available, the density was not measured. The calculated density, based on the empirical formula (see below), is 4.691 g cm^{-3}; the ideal chemical formula gives a calculated density of 4.528 g cm^{-3}. In the specimen studied, ferrostalderite has grown directly on dolomite and is associated with realgar, baumhauerite (?) and pyrite. Its crystallization is related to the activity of late-stage Tl-As-Cu-Fe-rich hydrothermal fluids during tectono-metamorphic Alpine events.

Chemical analysis

A preliminary chemical analysis using EDS performed on the crystal fragment used for the single-crystal X-ray diffraction experiment did not indicate the presence of elements ($Z > 9$) other than Fe, Cu, Zn, As, Ag, Hg, Tl and S. The same fragment was then analysed with a CAMECA SX 50 electron microprobe (wavelength dispersive spectrometry mode, accelerating voltage = 20 kV, beam current = 20 nA, beam size = 1–2 μm) available at the IGG-CNR Padova, Italy. Counting times were 20 s for peak and 15 s for background. The following standards (element, emission line) were used: Ag metal (Ag$L\alpha$), Cu metal (Cu$K\alpha$), sphalerite (Zn$K\alpha$, S$K\alpha$), Fe metal (Fe$K\alpha$), HgS (Hg$M\alpha$), Tl_2Se (Tl$M\alpha$), AsGa (As$L\alpha$), and Sb_2S_3 (Sb$L\alpha$). Cadmium, Se and Pb were sought but not found above detection limits (0.01 wt.%). Chemical data are given in Table 1. The relatively low total could be related to the small size of the polished grain.

TABLE 1. Microprobe analysis of ferrostalderite: chemical composition as wt.% and number of atoms on the basis of 12 atoms per formula unit (a.p.f.u.).

Element	wt.%	range	e.s.d.
Cu	6.24	5.98–6.47	0.25
Ag	4.18	4.09–4.26	0.09
Fe	9.95	8.99–10.48	0.83
Zn	4.46	3.88–5.50	0.91
Hg	1.22	0.99–1.50	0.26
Tl	26.86	26.24–27.48	0.62
As	19.05	18.88–19.24	0.18
Sb	0.63	0.56–0.68	0.06
S	25.39	24.85–25.72	0.47
Total	97.98	97.18–98.59	0.72
	a.p.f.u.	range	e.s.d.
Cu	0.749	0.728–0.773	0.023
Ag	0.296	0.287–0.301	0.008
Zn	0.521	0.449–0.651	0.113
Fe	1.359	1.245–1.421	0.099
Hg	0.046	0.037–0.058	0.011
Tl	1.003	0.993–1.018	0.013
As	1.941	1.914–1.986	0.039
Sb	0.040	0.035–0.043	0.004
S	6.044	5.995–6.076	0.043
Ev	–2.0	–3.2–0.2	1.9

Valence equilibrium: *Ev* (%) = [Σ(val+) – Σ(val–)] × 100/Σ(val–).

The only significant chemical variation (taking into account that only three spot analyses were performed, owing to the very small size of the studied grain) involves an inverse correlation between iron and zinc. On the basis of 12 atoms per formula unit (a.p.f.u.), the chemical formula of ferrostalderite is $Cu_{0.75(2)}Ag_{0.30(1)}Fe_{1.36(10)}Zn_{0.52(11)}Hg_{0.05(1)}Tl_{1.00(1)}[As_{1.94(4)}Sb_{0.04(1)}]_{\Sigma 1.98(4)}S_{6.04(4)}$.

Crystallography

For the X-ray single-crystal studies, intensity data were collected using a Supernova (Agilent Technologies) diffractometer equipped with a Mova micro-source (spot size = 0.120 mm, Mo$K\alpha$ radiation) combined with a Pilatus 200 K detector (Dectris), at the Department of Geosciences, University of Padova, Italy. The detector-to-crystal distance was 68 mm and 2592 frames were collected with the ω scan mode, in 1° slices, with an exposure time of 10 s per frame. Intensity integration and standard Lorentz-polarization corrections were performed with the *CrysAlis RED* (Oxford Diffraction, 2006) software package. The program *ABSPACK* in *CrysAlis RED* (Oxford Diffraction, 2006) was used for the absorption correction. Statistical tests on the distribution of $|E|$ values ($|E^2 - 1| = 0.584$) and the systematic absences suggested the space group $I\bar{4}2\,m$. The refined unit-cell parameters are a = 9.8786(5), c = 10.8489(8) Å, V = 1058.71(11) Å^3.

The crystal structure of ferrostalderite was refined starting from the atom coordinates given by Bindi (2008) for routhierite, using *Shelxl-97* (Sheldrick, 2008). Scattering curves for neutral atoms were taken from the *International Tables for*

TABLE 2. Crystal and experimental data for ferrostalderite.

Crystal data	
Crystal size (mm)	0.010 × 0.020 × 0.040
Cell setting, space group	Tetragonal, $I\bar{4}2m$
a, c (Å);	9.8786(5), 10.8489(8)
V (Å^3)	1058.71(11)
Z	4
Data collection and refinement	
Radiation, wavelength (Å)	Mo$K\alpha$, λ = 0.71073
Temperature (K)	293
$2\theta_{max}$ (°)	69.92
Measured reflections	28,463
Unique reflections	1258
Reflections with $F_o > 4\sigma(F_o)$	1169
R_{int}	0.0951
$R\sigma$	0.0324
Range of h, k, l	$-15 \le h \le 15$, $-15 \le k \le 15$, $-17 \le l \le 17$
R [$F_o > 4\sigma(F_o)$]	0.0496
R (all data)	0.0545
wR (on F^2)	0.1106
Gof	1.172
Number of least-squares parameters	38
Maximum and minimum residual peak (e Å^{-3})	3.04 (at 0.91 Å from Tl) –3.03 (at 0.36 Å from Tl)

Crystallography (Wilson, 1992). Crystal data and details of intensity data collection and refinement are reported in Table 2. After several cycles of isotropic refinement, R_1 converged to 0.115, suggesting the validity of the structural model. Four independent cation sites occur in the crystal structure of ferrostalderite, labelled Tl, *M*1, *M*2 and As. *M*1 and *M*2 sites correspond to Cu and Hg sites in the crystal structure of routhierite (Bindi, 2008; Biagioni *et al*., 2014*a*). The occupancies of these four independent cation sites were refined using the following scattering curves: Tl site: Tl *vs.* □ (vacancy); *M*1 site: Cu *vs.* □; *M*2 site: Ag *vs.* □; As site: As *vs.* □. The Tl site was found to be fully occupied by Tl and its site occupancy was fixed to 1. At the *M*1 and *M*2 sites the refined site-scattering values are 27.2 and 31.9 electrons, whereas at the As site a near-pure As occupancy was observed (33.3 electrons). Final atom coordinates and displacement parameters are given in Table 3, whereas selected bond distances are reported in Table 4. Table 5 gives the refined and calculated site scattering (in electrons per formula unit, e.p.f.u.) on the basis of the proposed site populations (see below). Iron has been considered as divalent, as in the other members of the routhierite isotypic series; this is consistent with the observation of Makovicky *et al*. (1990) that the presence of Zn and Hg favours Fe^{2+} with respect to Fe^{3+}. Table 6 shows the results of the bond valence calculations.

Owing to the very small size and the few available crystals, obtaining a powder X-ray diffraction pattern was not attempted. Table 7 reports the calculated powder X-ray diffraction data of ferrostalderite on the basis of the crystallographic data collected through single-crystal X-ray diffraction.

Crystal structure description

The crystal structure of ferrostalderite is isotypic with those of the other members of the routhierite isotypic series (Graeser *et al*., 1995; Bindi, 2008; Biagioni *et al*., 2014*a*,*b*; Bindi *et al*., 2015*b*), showing a framework formed by two independent MeS_4 tetrahedra sharing corners, hosting channels parallel to [001]. These channels contain TlS_6 and $(As,Sb)S_3$ polyhedra, sharing corners and edges with the tetrahedron framework (Fig. 2).

As stated above, four independent cation sites occur. The two independent tetrahedral sites, *M*1 and *M*2, have average bond distances of 2.332 and 2.385 Å, respectively. The <*M*1–S> bond distance is a little shorter than that observed by Graeser *et al*.

TABLE 3. Atom coordinates and displacement parameters (Å^2) for ferrostalderite.

Site	Wyckoff site	*x/a*	*y/b*	*z/c*	U_{eq}	U^{11}	U^{22}	U^{33}	U^{23}	U^{13}	U^{12}
Tl	4*e*	0	0	0.34889(6)	0.0479(3)	0.0593(4)	0.0593(4)	0.0252(3)	0	0	–0.0178(5)
*M*1	4*d*	0	½	¼	0.0210(5)	0.0149(5)	0.0149(5)	0.0333(9)	0	0	0
*M*2	8*f*	0.2241(1)	½	½	0.0256(3)	0.0325(6)	0.0222(5)	0.0220(5)	–0.0009(5)	0	0
As	8*i*	0.26343(7)	0.26343(7)	0.2486(2)	0.0180(3)	0.0172(3)	0.0172(3)	0.0196(4)	0.0009(3)	0.0009(3)	–0.0003(3)
S1	16*j*	0.1017(2)	0.3410(2)	0.3790(2)	0.0207(3)	0.0200(8)	0.0201(8)	0.0214(8)	–0.0016(6)	0.0021(7)	0.0054(6)
S2	8*i*	0.1287(2)	0.1287(2)	0.1300(2)	0.0213(5)	0.0230(8)	0.0230(8)	0.0176(11)	–0.0018(6)	–0.0018(6)	–0.0019(8)

TABLE 4. Selected bond distances (Å) in ferrostalderite.

Tl – S2	2.979(3) × 2	*M*1 – S1	2.332(2) × 4
– S1	3.530(2) × 4		
average	3.346		
As – S1	2.268(2) × 2	*M*2 – S1	2.377(2) × 2
– S2	2.280(3)	– S2	2.392(2) × 2
average	2.272	average	2.385

(1995) for the Cu site of stalderite and by Bindi *et al*. (2015*b*) for ralphcannonite, i.e. 2.357(4) and 2.358(7) Å, respectively. Similarly, the <*M*2–S> bond distance is shorter than those reported at the *M*2 site of ralphcannonite (2.468 Å) and at the Zn site of stalderite (2.406 Å). Whereas in other members of the routhierite isotypic series the *M*2 tetrahedron is distorted, with two relatively short and two relatively long bonds, in ferrostalderite the coordination is quite regular, with bond distances of 2.377(2) and 2.392(2) Å. The As site forms a trigonal pyramid with three S atoms, with an average bond distance of 2.272 Å. The refinement of the site occupancy points to the dominant occupancy of this site by arsenic, with only a negligible amount of Sb, in agreement with chemical data showing only 0.03 Sb a.p.f.u. The coordination of the Tl site can be described as an orthorhombic pyramid with a split apex, as in the other members of the routhierite isotypic series. On the other side of the split apex, a relatively short Tl–Tl distance occurs, i.e. 3.279(1) Å. This value perfectly agrees with that reported for stalderite (3.28 Å) by Graeser *et al*. (1995), being in the range of Tl–Tl distances observed in other members of the routhierite group. Such a short distance is most likely indicative of some type of Tl–Tl interaction, as observed in other Tl compounds, e.g. christite (Brown and Dickson, 1976) and gabrielite (Balić-Žunić *et al*., 2006).

Site population and bond valence balance

The similar scattering factors of Fe (Z = 26), Cu (Z = 29) and Zn (Z = 30) do not permit accurate knowledge of their partitioning between the two tetrahedral sites *M*1 and *M*2 by using conventional Mo$K\alpha$ radiation only. Consequently, some additional considerations based on average bond distances and bond-valence sums are required. Since the description of arsiccioite (Biagioni *et al*., 2014*b*), it has become clear that the steric effect has

TABLE 5. Refined site-scattering values (e.p.f.u.), assigned site population (a.p.f.u.) with corresponding calculated site-scattering (e.p.f.u.), and comparison between observed and calculated bond distances (in Å) at *M*1, *M*2 and As sites in ferrostalderite.

Site	Refined site-scattering values	Assigned site population	Calculated site-scattering	$\langle Me–S\rangle_{obs}$	$\langle Me–S\rangle_{calc}$
*M*1	27.0	$Cu_{0.75}Zn_{0.25}$	29.2	2.332	2.364
*M*2	31.8	$Fe_{0.68}Ag_{0.15}Zn_{0.14}Hg_{0.03}$	31.3	2.385	2.448
As	33.1	$As_{0.98}Sb_{0.02}$	33.4	2.272	2.264

TABLE 6. Bond-valence sums (BVS, in valence units, vu) calculated using the parameters given by Brese and O'Keeffe (1991).*

	*M*1	*M*2	Tl	As	Σ anions
S1	$0.34^{\times 4}$	$0.55^{\times 2}$	$0.09^{\times 4}$	$0.99^{\times 2}$	1.97
S2		$^{2\times}0.53^{\times 2}$	$0.39^{\times 2}$	0.96	2.41
Σ cations	1.36	2.16	1.13	2.94	
Theor.	1.25	1.85	1.00	3.00	

*In mixed sites, the bond-valence contribution of each cation has been weighted according to its site-population (see Table 5). Left and right superscripts indicates the number of bonds involving cations and anions, respectively.

priority over the valence state in governing the metal distribution between *M*1 and *M*2 sites in routhierite isotypes. This observation has been confirmed by the structure refinement of ralphcannonite (Bindi *et al.*, 2015*b*). As a consequence, Ag has been attributed to the *M*2 site in the crystal structure of ferrostalderite and the substitution $^{M1}Cu^{+} + {}^{M2}(Fe, Zn,Hg)^{2+} \rightarrow {}^{M1}Zn^{2+} + {}^{M2}Ag^{+}$ is assumed to take place. In addition, and notwithstanding the very low number of spot analyses (only three, as discussed

TABLE 7. Calculated powder X-ray diffraction data for ferrostalderite.*

I_{calc}	d_{calc}	*h k l*	I_{calc}	d_{calc}	*h k l*
12	6.985	1 1 0	7	2.340	4 1 1
10	5.424	0 0 2	10	2.184	3 2 3
8	4.939	2 0 0	14	2.048	3 1 4
70	**4.092**	**2 1 1**	17	1.997	4 1 3
23	**3.493**	**2 2 0**	10	1.845	4 0 4
35	**3.396**	**1 0 3**	13	1.826	4 0 4
17	3.124	3 1 0	13	1.809	5 2 1
100	**2.937**	**2 2 2**	16	1.746	4 4 0
9	2.798	2 1 3	8	1.734	4 3 3
19	**2.656**	**3 2 1**	9	1.713	4 2 4
13	2.528	1 1 4	7	1.606	6 1 1
19	**2.470**	**4 0 0**	7	1.576	5 1 4
33	**2.435**	**3 0 3**	5	1.565	3 1 6
12	2.377	2 0 4	13	1.501	6 2 2

*Intensity and d_{hkl} were calculated using the software *Powdercell 2.3* (Kraus and Nolze, 1996) on the basis of the structural model given in Table 3; only reflections with $I_{calc} > 5$ are listed. The seven strongest reflections are given in bold.

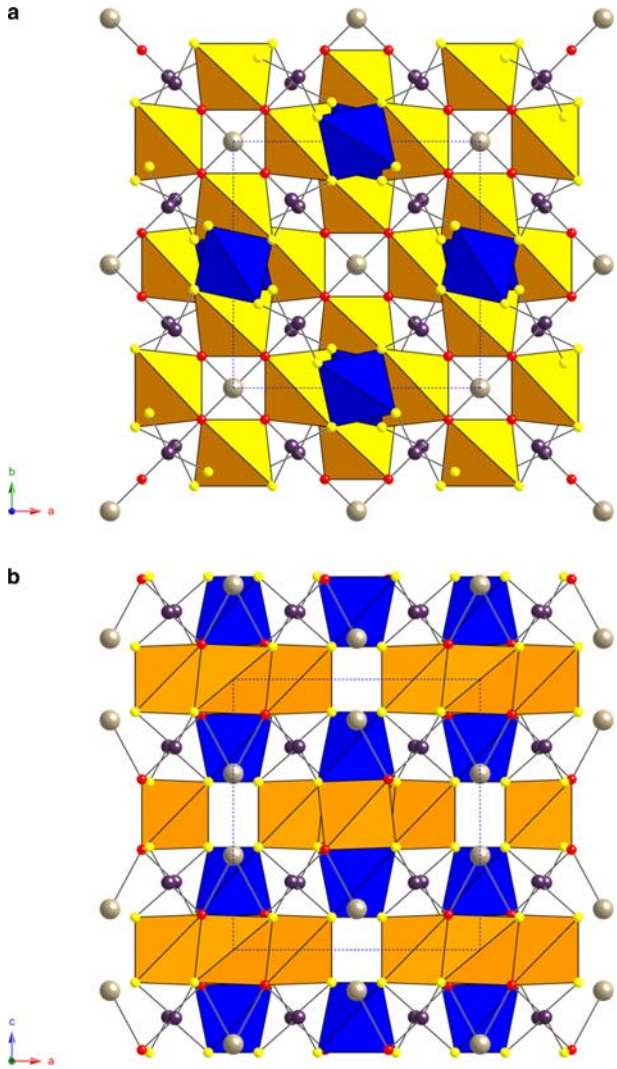

FIG. 2. Crystal structure of ferrostalderite, as seen down [001] (*a*) and [010] (*b*). Polyhedra are: blue: *M*1 tetrahedra; orange: *M*2 tetrahedra. Circles are grey: Tl site; violet: As site; yellow: S1 site; red: S2 site.

above), a negative correlation between Fe^{2+} and (Zn^{2+}+Hg^{2+}) was observed (Fig. 3), in agreement with the data for stalderite given by Graeser *et al.* (1995). This suggests that the homovalent substitution $(Zn,Hg)^{2+} \rightarrow Fe^{2+}$ takes place at the *M*2 site, which gives the site population in Table 5. The calculated site-scattering values (e.p.f.u.) are compared with refined site scattering, whereas observed average <*Me*–S> bond distances are compared with those calculated. According to the parameters given by Brese and O'Keeffe (1991), the ideal *Me*–S distance (in Å) decreases according to the sequence 2.663/Ag^{+}, 2.576/Hg^{2+}, 2.416/Fe^{2+}, 2.370/Cu^{+} and 2.346/Zn^{2+}.

The bond-valence sums (BVS) were calculated by using the parameters given by Brese and O'Keeffe (1991) and are reported in Table 6. As with some other members of the routhierite isotypic series (e.g. arsiccioite – Biagioni *et al.*, 2014*b*; ralphcannonite – Bindi *et al.*, 2015*b*), significant deviations from the expected values were observed (up to +17%), in particular at the *M*2 site, which appears smaller than expected, resulting in an overbonding of the hosted metals. Overbonding at

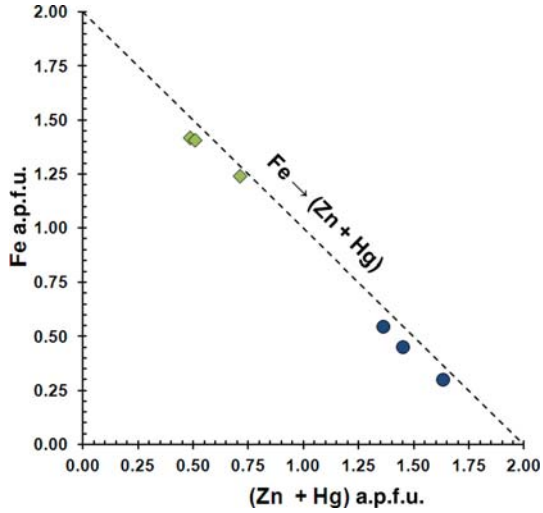

FIG. 3. (Zn + Hg) content (in a.p.f.u.) *vs*. Fe content in the pair stalderite (blue circles) – ferrostalderite (green diamonds). Data for stalderite are after Graeser *et al.* (1995).

the metal sites influences the BVS of the S atoms, particularly that occupying the S2 position, having a strong BVS excess (corresponding to +20.5% with respect to the expected value, i.e. 2 valence units, vu). A BVS excess similar to those reported in other routhierite isotypes occurs also for the Tl atom. On the contrary, quite good agreement between calculated and expected BVS at the As site was obtained. The reason for the BVS excess at the metal sites could possibly be related to the overestimation of bond parameters for some (*Me*,S) pairs by Brese and O'Keeffe (1991), as discussed briefly for the (Tl,S) pair by Biagioni *et al*. (2014*b*). For example, by using these parameters, an ideal <Ag–S> tetrahedral bond distance of 2.663 Å can be calculated. It should be noted that in some compounds having Ag in tetrahedral coordination, the bond distance of the pure Ag site is shorter than ideal. For example, the synthetic compound Ag_2HgGeS_4 (Parasyuk *et al*., 2002) has two Ag tetrahedral sites. The first has a pure Ag population and shows an average bond distance of 2.56 Å; the other site has a mixed ($Ag_{0.5}Hg_{0.5}$) site occupancy, with an average bond distance of 2.55 Å. Consequently, the pure Ag site does not appear significantly larger than the mixed (Ag,Hg) one, contrasting with the assumption that <Ag–S> has a significantly larger bond distance than <Hg–S>.

The crystal chemical formula of ferrostalderite can be written as $^{M1}(Cu_{0.75}Zn_{0.25})^{M2}(Fe_{0.68}Ag_{0.15}Zn_{0.14}Hg_{0.03})_2Tl(As_{0.98}Sb_{0.02})_2S_6$, with the relative error of the valence equilibrium *Ev* (%) = –0.42.

Discussion

Crystal chemistry of ferrostalderite in the framework of the routhierite isotypic series

Ferrostalderite, ideally $^{M1}Cu^{M2}Fe_2TlAs_2S_6$, is the Fe analogue of stalderite and routhierite (Fig. 4). So far, the divalent metal ions found in the routhierite isotypic series are Fe^{2+}, Hg^{2+} and Zn^{2+}. The latter seems to play a central role in this series, being widely substituted by both Fe and by Hg, as occurs in other compounds having a sphalerite-related structure, e.g. the tetrahedrite isotypes (Moëlo *et al*., 2008). Whereas the substitutions $Zn^{2+} \rightarrow Fe^{2+}$ and $Zn^{2+} \rightarrow Hg^{2+}$ are widely represented in minerals, available data suggest a more limited $Fe^{2+} \rightarrow Hg^{2+}$ substitution (e.g. a new potential fettelite-like mineral; Bindi *et al*., 2012). These considerations are in keeping with the finding of a relatively wide compositional range between stalderite and ferrostalderite (taking into account the small amount of available chemical data) and a very limited solid solution between the latter and routhierite. Interestingly, a higher Zn content seems to favour the incorporation of Hg in the crystal structure of these compounds, in agreement with the crystal chemistry of other sphalerite-related compounds.

The crystallization of the different members of the routhierite isotypic series is probably mainly controlled by the geochemistry of the mineralizing fluids. In Hg-rich environments (e.g., Monte Arsiccio mine, Tuscany, Italy – Biagioni *et al*.,

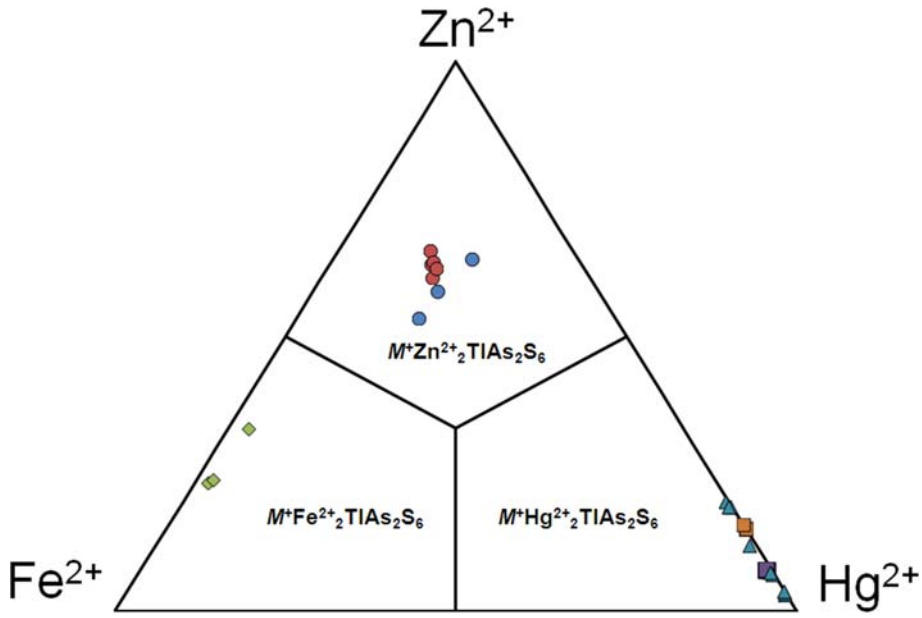

FIG. 4. Chemical composition of the members of the routhierite isotypic series, $M^{+}M_2^{2+}TlAs_2S_6$. Symbols: light blue triangles = arsiccioite; violet squares = routhierite from Monte Arsiccio mine; orange squares = routhierite from Jas Roux; blue circles = stalderite; red circles = ralphcannonite; green diamonds = ferrostalderite. Chemical data are after Biagioni *et al.* (2014*a*,*b*), Bindi (2008), Bindi *et al.* (2015*b*), Graeser *et al.* (1995) and Johan *et al.* (1974).

2013; Jas Roux, Haute-Alpes, France – Johan and Mantienne, 2000), routhierite and arsiccioite crystallized, differing by the Ag-dominant nature of the latter; the same relationship is displayed by the pair stalderite–ralphcannonite, crystallizing in Hg-poor environments (e.g. Lengenbach, Binn Valley, Switzerland – Graeser *et al*., 2008; Roth *et al*., 2014). An increasing amount of Ag promotes a shift in the crystal chemical formula from $^{M1}Me^{+M2}Me_2^{2+}TlAs_2S_6$ (routhierite and stalderite) to $^{M1}Me^{2+M2}(Me_{0.5}^{+}Me_{0.5}^{2+})_2TlAs_2S_6$ (arsiccioite and ralphcannonite). It is not clear if an Ag analogue of ferrostalderite could exist. In fact, the atomic radius of Fe^{2+} is larger than those of Zn^{2+} and Cu^{+} and so it is not clear if the *M*1 site could host this metal as a consequence of Ag incorporation at the *M*2 position.

Iron in sulfosalts

Among sulfosalts, few mineral species contain Fe as an essential constituent (Table 8). Iron shows two different coordination environments, being hosted in tetrahedral as well as octahedral polyhedra, the former generally occurring in sphalerite-related structures. Tetrahedral coordination, similar to that observed in ferrostalderite, was reported in members of the tetrahedrite isotypic series (e.g. Andreasen *et al*., 2008). In ferrostalderite as well as in the tetrahedrite isotypes, Fe occurs in tetrahedral sites having mixed occupancy, usually represented by zinc and, rarely, by mercury. An additional species is miharaite, an unclassified Cu sulfosalt of which the crystal structure was solved by Petrova *et al*. (1988). Iron is tetrahedrally coordinated, with bond distances ranging between 2.30 and 2.37 Å, with an average value of 2.33 Å.

Octahedral coordination of iron has been reported in sulfosalts belonging to the berthierite isotypic series (berthierite and garavellite), in the well-known lead-antimony sulfosalt jamesonite, and in members of the cylindrite homologous series. In berthierite and garavellite the average <Fe–S> bond distances are 2.53 and 2.54 Å, respectively (Buerger and Hahn, 1955; Lemoine *et al*., 1991; Lukaszewicz *et al*., 2001; Bindi and Menchetti, 2005); a very similar <Fe–S> bond distance has been observed in jamesonite, i.e. 2.56 Å (Léone *et al*., 2003). Finally, iron is an essential constituent in coiraite, cylindrite and franckeite, species belonging to the cylindrite group of complex Pb sulfosalts, as proved by

TABLE 8. Iron coordination number (C.N.) and chemical formulae of sulfosalts having Fe as an essential constituent.

C.N.	Group	Mineral species	Chemical formula
IV	Tetrahedrite isotypic series	Argentotetrahedrite	$Ag_6[Ag_4(Fe,Zn)_2]Sb_4S_{13}$
		Argentotennantite	$Ag_6[Cu_4(Fe,Zn)_2]As_4S_{13}$
		Freibergite	$Ag_6[Cu_4Fe_2]Sb_4S_{13}$
		Giraudite	$Cu_6[Cu_4(Fe,Zn)_2]As_4Se_{13}$
		Tennantite	$Cu_6[Cu_4(Fe,Zn)_2]As_4S_{13}$
		Tetrahedrite	$Cu_6[Cu_4(Fe,Zn)_2]Sb_4S_{13}$
	Routhierite isotypic series	Ferrostalderite	$CuFe_2TlAs_2S_6$
	Unclassified Cu sulfosalt	Miharaite	$Cu_4FePbBiS_6$
VI	Berthierite isotypic series	Berthierite	$FeSb_2S_4$
		Garavellite	$FeSbBiS_4$
	Cylindrite homologous series	Cylindrite	$FePb_3Sn_4Sb_2S_{14}$
		Coiraite	$Fe(Pb,Sn)_{12.5}Sn_5As_3S_{28}$
		Franckeite	$Fe(Pb,Sn)_6Sn_2Sb_2S_{14}$
	Jamesonite isotypic series	Jamesonite	$FePb_4Sb_6S_{14}$

some experimental syntheses (Sachdev and Chang, 1975; Li, 1984). These minerals have an incommensurate composite-layered structure, formed by the regular stacking of two kinds of layers, a pseudotetragonal *Q* layer and a pseudohexagonal *H* layer. Owing to the incommensurate layered structure of these phases, structural data are poor. Whereas the crystal structure of franckeite has been solved recently by Makovicky *et al*. (2011), those of cylindrite and coiraite have not. However, the crystal structure of a synthetic Sn-Se representative of the cylindrite structure type has been described by Makovicky *et al*. (2008). Consequently, it has been observed that in franckeite and cylindrite, iron is partitioned within the *H* layers, in an octahedral environment. Owing to the relationships with the other phases of the cylindrite homologous series, Paar *et al*. (2008) assumed the same iron partitioning within the *H* layers of coiraite.

Conclusion

The complex crystal chemistry shown by the members of the routhierite isotypic series, strongly influenced by the geochemistry of the crystallization environment, has, in recent years, favoured the description of three new mineral species, arsiccioite, ralphcannonite and ferrostalderite. The latter represents a new kind of Fe sulfosalt and increases the number of thallium minerals described from the Lengenbach dolostone. Indeed, ferrostalderite is the twentieth thallium species described from this Swiss locality and confirms its exceptional status as a hotspot for the study of sulfosalt assemblages in a metamorphic environment. Lengenbach appears as the most productive field, today, for sulfosalt systematics.

Acknowledgements

This research was supported by "Progetto d'Ateneo 2012. Università di Firenze" to LB. Comments by Chris J. Stanley, Peter Leverett and Stefan Graeser helped to improve the paper. Pete Williams is thanked for efficient handling of the manuscript and useful comments.

References

Andreasen, J.W., Makovicky, E., Lebech, B. and Karup-Møller, S. (2008) The role of iron in tetrahedrite and tennantite determined by Rietveld refinement of neutron powder diffraction data. *Physics and Chemistry of Minerals*, **35**, 447–454.

Balić-Žunić, T., Makovicky, E., Karanović, L., Poleti, D. and Graeser, S. (2006) The crystal structure of gabrielite, $Tl_2AgCu_2As_3S_7$, a new species of thallium sulfosalt from Lengenbach, Switzerland. *The Canadian Mineralogist*, **44**, 141–158.

Biagioni, C., D'Orazio, M., Vezzoni, S., Dini, A. and Orlandi, P. (2013) Mobilization of Tl-Hg-As-Sb-(Ag, Cu)-Pb sulfosalt melts during low-grade metamorphism in the Alpi Apuane (Tuscany, Italy). *Geology*, **41**, 747–751.

Biagioni, C., Bonaccorsi, E., Moëlo, Y. and Orlandi, P. (2014*a*) Mercury-arsenic sulfosalts from Apuan Alps (Tuscany, Italy). I. Routhierite, $(Cu_{0.8}Ag_{0.2})Hg_2Tl(As_{1.4}Sb_{0.6})_{\Sigma=2}S_6$, from Monte Arsiccio mine: occurrence and crystal structure. *European Journal of Mineralogy*, **26**, 163–170.

Biagioni, C., Bonaccorsi, E., Moëlo, Y., Orlandi, P., Bindi, L., D'Orazio, M. and Vezzoni, S. (2014*b*) Mercury-arsenic sulfosalts from the Apuan Alps (Tuscany, Italy). II. Arsiccioite, $AgHg_2TlAs_2S_6$, a new mineral from the Monte Arsiccio mine: occurrence, crystal structure and crystal chemistry of the routhierite isotypic series. *Mineralogical Magazine*, **78**, 101–117.

Bindi, L. (2008) Routhierite, $Tl(Cu,Ag)(Hg,Zn)_2(As,Sb)_2S_6$. *Acta Crystallographica*, **C64**, i95–i96.

Bindi, L. and Menchetti, S. (2005) Garavellite, $FeSbBiS_4$, from the Caspari mine, North Rhine-Westphalia, Germany: composition, physical properties and determination of the crystal structure. *Mineralogy and Petrology*, **85**, 131–139.

Bindi, L., Downs, R.T., Spry, P.G., Pinch, W.W. and Menchetti, S. (2012) A chemical and structural re-examination of fettelite samples from the type locality, Odenwald, southwest Germany. *Mineralogical Magazine*, **76**, 551–566.

Bindi, L., Biagioni, C., Nestola, F., Cannon, R., Roth, P. and Raber, T. (2015*a*) Ferrostalderite, IMA 2014–090. CNMNC Newsletter No. 24, April 2015, page 248; *Mineralogical Magazine*, **79**, 247–251.

Bindi, L., Biagioni, C., Raber, T., Roth, P. and Nestola, F. (2015*b*) Ralphcannonite, $AgZn_2TlAs_2S_6$, a new mineral of the routhierite isotypic series from Lengenbach, Binn Valley, Switzerland. *Mineralogical Magazine*, **79**, 1089–1098.

Brese, N.E. and O'Keeffe, M. (1991) Bond-valence parameters for solids. *Acta Crystallographica,* **B47**, 192–197.

Brown, K.L. and Dickson, F.W. (1976) The crystal structure of synthetic christite, $HgTlAsS_3$. *Zeitschrift für Kristallographie*, **144**, 367–376.

Buerger, M.J. and Hahn, T. (1955) The crystal structure of berthierite, $FeSb_2S_4$. *American Mineralogist*, **40**, 226–238.

Graeser, S., Schwander, H., Wulf, R. and Edenharter, A. (1995) Stalderite, $TlCu(Zn,Fe,Hg)_2As_2S_6$ – a new mineral related to routhierite: description and crystal structure. *Schweizerische Mineralogische und Petrographische Mitteilungen*, **75**, 337–345.

Graeser, S., Cannon, R., Drechsler, E., Raber, T. and Roth, P. (2008) *Faszination Lengenbach Abbau-Forschung-Mineralien 1958–2008.* Kristallographik Verlag, Achberg, Germany.

Hofmann, B.A. and Knill, M.D. (1996) Geochemistry and genesis of the Lengenbach Pb-Zn-As-Tl-Ba mineralization, Binn Valley, Switzerland. *Mineralium Deposita*, **31**, 319–339.

Johan, Z. and Mantienne, J. (2000) Thallium-rich mineralization at Jas Roux, Hautes-Alpes, France: a complex epithermal, sediment-hosted, ore-forming system. *Journal of the Czech Geological Society*, **45**, 63–77.

Johan, Z., Mantienne, J. and Picot, P. (1974) La routhiérite, $TlHgAsS_3$, et la laffittite, $AgHgAsS_3$, deux nouvelles espèces minerales. *Bulletin de la Société française de Minéralogie et de Cristallographie*, **97**, 48–53.

Kraus, W. and Nolze, G. (1996) PowderCell – a program for the representation and manipulation of crystal structures and calculation of the resulting X-ray powder patterns. *Journal of Applied Crystallography*, **29**, 301–303.

Lemoine, P.P., Carré, D. and Robert, F. (1991) Structure du sulfure de fer et d'antimoine, $FeSb_2S_4$ (berthierite). *Acta Crystallographica*, **C47**, 938–940.

Léone, P., Le Leuch, L.M., Palvadeau, P., Molinie, P. and Moëlo, Y. (2003) Single crystal structure and magnetic properties of two iron or manganese-lead-antimony sulfides: $MPb_4Sb_6S_{14}$ (M:Fe, Mn). *Solid State Sciences*, **5**, 771–776.

Li, J. (1984) Franckeite syntheses and heating experiments. *Neues Jahrbuch für Mineralogie, Abhandlungen*, **150**, 45–50.

Lukaszewicz, K., Pietraszko, A., Stepien-Damm, J., Kajokas, A., Grigas, J. and Drulis, H. (2001) Crystal structure, Mössbauer spectra, thermal expansion, and phase transition of berthierite, $FeSb_2S_4$. *Journal of Solid State Chemistry*, **162**, 79–83.

Makovicky, E., Forcher, K., Lottermoser, W. and Amthauer, G. (1990) The role of Fe^{2+} and Fe^{3+} in synthetic Fe-substituted tetrahedrite. *Mineralogy and Petrology*, **43**, 73–81.

Makovicky, E., Petříček, V., Dušek, M. and Topa, D. (2008) Crystal structure of a synthetic tin-selenium representative of the cylindrite structure type. *American Mineralogist*, **93**, 1787–1798.

Makovicky, E., Petříček, V., Dušek, M. and Topa, D. (2011) The crystal structure of franckeite, $Pb_{21.7}Sn_{9.3}Fe_{4.0}Sb_{8.1}S_{56.9}$. *American Mineralogist*, **96**, 1686–1702.

Moëlo, Y., Makovicky, E., Mozgova, N.N., Jambor, J.L., Cook, N., Pring., A., Paar, W.H., Nickel, E.H., Graeser, S., Karup-Møller, S., Balić-Žunić, T., Mumme, W.G., Vurro, F., Topa, D., Bindi, L., Bente, K. and Shimizu, M. (2008) Sulfosalt systematics: a review. Report of the sulfosalt sub-committee of the IMA Commission on Ore Mineralogy. *European Journal of Mineralogy*, **20**, 7–46.

Oxford Diffraction (2006) *CrysAlis RED (Version 1.171.31.2) and ABSPACK in CrysAlis RED.* Oxford Diffraction Ltd, Abingdon, UK.

Paar, W.H., Moëlo, Y., Mozgova, N.N., Organova, N.I., Stanley, C.J., Roberts, A.C., Culetto, F.J., Effenberger, H.S., Topa, D., Putz, H., Sureda, R.J. and de Brodtkorb,

M.K. (2008) Coiraite, $(Pb,Sn^{2+})_{12.5}$ $As_3Fe^{2+}Sn_5^{4+}S_{28}$: a franckeite-type new mineral from Jujuy Province, NW Argentina. *Mineralogical Magazine*, **72**, 1083–1101.

Parasyuk, O.V., Gulay, L.D., Piskach, L.V. and Gagalovska, O.P. (2002) The Ag_2S-HgS-GeS_2 system at 670 K and the crystal structure of the Ag_2HgGeS_4 compound. *Journal of Alloys and Compounds*, **336**, 213–217.

Petrova, I.V., Pobedimskaya, E.A. and Bryzgalov, I.A. (1988) Crystal structure of miharaite $Cu_4FePbBiS_6$. *Doklady Akademii Nauk SSSR*, **299**, 123–127 [in Russian].

Roth, P., Raber, T., Drechsler, E. and Cannon, R. (2014) The Lengenbach Quarry, Binn Valley, Switzerland. *The Mineralogical Record*, **45**, 157–196.

Sachdev, S.C. and Chang, L.L.Y. (1975) Phase relations in the system tin-antimony-lead sulfides and the synthesis of cylindrite and franckeite. *Economic Geology*, **70**, 1111–1122.

Sheldrick, G.M. (2008) A short history of SHELX. *Acta Crystallographica*, **A64**, 112–122.

Wilson, A.J.C. (1992) *International Tables for X-ray Crystallography Volume C*. Kluwer, Dordrecht, The Netherlands.